LAB-TO-FIELD SCALING OF TWO-PHASE FLOW IN THE WELLBORE REGION

S.A. Betata* and J.-C. Moulu**

* Ministère de l'Energie et des Mines, Alger, Algérie
** Institut Français du Pétrole, Rueil-Malmaison, France

ABSTRACT

During the production phase of an oil reservoir, a pressure drawdown occurs in the near wellbore region. This may lower the pressure below the bubble-point pressure, leading to the appearance of a gas phase, thus decreasing the oil relative permeability and the well productivity.

The main goal of this study is the development of an appropriate laboratory procedure and its modelling, so as to derive gas-oil relative permeabilities at conditions representative of the near wellbore region, e.g. for a dispersed gas phase.

A set of depressurization tests in porous media are performed for various conditions of pressure gradient and supersaturation. They are interpreted using a model relating the gas saturation to the supersaturation, as well as the nucleation rate J.

Gas-oil relative permeabilities and average gas saturation versus time are measured. Oil relative permeabilities are found to be a function of both the gas saturation and the supersaturation. In addition to that, above a given threshold pressure drop part of the gas is mobilized. The value of J, obtained from the oil production curve, leads to the description of the bubble population, in terms of their number and size. It is shown that oil-phase flow impairment is caused more by a limited number of large bubbles rather than by the presence of regularly distributed small ones.

The procedure thus established allows the description of the behavior of oil and gas, not only above the critical gas saturation (defined as the saturation above which the gas phase becomes continuous), but also in the early stage of the nucleation, when the gas, even in a dispersed form, can flow depending on the applied pressure gradient.

INTRODUCTION

During the lifetime of a reservoir, its pressure may fall below the bubble point pressure. A gaseous phase appears, due to nucleation of the initially dissolved gas, in the form of small bubbles growing up by diffusion. This phenomenon may affect the whole reservoir, and oil can spontaneously be produced. The oil thus recovered corresponds to the volume of the liberated gas (primary recovery). The production is economically feasible as long as the gas phase has not reached the critical gas saturation, S_{gc}, above which the gas phase becomes continuous, reaching the producing well .

On the other hand, the phenomenon can be limited only to the wellbore region, where the pressure profile may be partly below the bubble point pressure. Then a two-phase flow develops and the oil mobility decreases, inducing a great productivity reduction. The knowledge of the flow characteristics, such as relative permeabilities, in this area is then very

important for the reservoir engineer. Moreover, the notion of critical gas saturation may have a different meaning, since, due to the high pressure gradient developed, at least a part of the gas phase can be mobilized, even though discontinuous.

It is well-known that the relative permeability measured from an external gas drive test is likely to be different from that for a solution gas drive [1,2]. This difference in oil flow behavior is often attributed to the complex nature of the pore space and to the fact that the source of gas for the two types of displacements is not the same. In a solution gas drive, the gas is liberated from oil within the pores, even in the very small ones, while in an external drive the gas is injected from an outside source and cannot reach some of the low permeability zones of the rock. However, information on directly measured solution-gas-drive relative permeability is not available, and thus relative permeabilities from external gas drive are often used. The difference between solution gas drive and external injection relative permeabilities is important in the case of heterogeneous low permeability porous media[2]. An important issue concerning the oil/gas relative permeabilities during primary depletion, is the critical gas saturation and how it should be measured. The literature [3,4,5] strongly suggests that the critical gas saturation for a solution gas drive may be different from the value measured by external gas drive tests. In spite of some attempts [6] and because of a lack of information, the critical gas saturation from the external gas drive test is often used in numerical models [7].

The main goal of this study is the development of an appropriate laboratory procedure and its modelling to derive gas-oil relative permeabilities at conditions representative of the near wellbore region, e.g. for a dispersed gas phase. With the aim to perform experiments in the more simplest conditions, the rock and fluids of an actual reservoir are replaced by outcrop cores and a synthetic mixture.

The paper is organized as follows : (a) flow experiments performed at conditions corresponding to the wellbore region are described, and the relative permeabilties to oil and gas are measured; (b) nucleation is studied, first in a general way in a micromodel, and after that, more specifically with the porous medium and the fluids assumed to come from the reservoir. The description of the bubble population is deduced at static conditions and in the presence of the reservoir pressure gradient giving the final gas saturation value ; and (c) the results are interpreted and a correlation is found between the residual bubble population and the final relative permeability of oil.

FLOW EXPERIMENTS

Description of the wellbore region and experiments performed

Darcy's law applied to a radial structure gives the value of the pressure and supersaturation around the producing well for a given productivity (0.4 m^3 / h / m^2 of well surface corresponding typically to a well of Hassi-Messaoud). The results show that, if the pressure in the well is taken as the reference one, the pressure in the reservoir grows up slowly and reaches only 3 bar at a distance of 100 m from the well. Then, the maximum supersaturation pressure is 4.06 bar in the vicinity of the well (of radius 10 cm). Taking these values into account, the laboratory pressure drop will be relatively low : only 0.83 bar if the sample (Length = 60 cm) is assumed to be placed close to the well. These low values correspond to

the flow of an oil having a low viscosity (0.20 cp), therefore, it is likely that the pressure drop around a well would be much higher in the case of a viscous oil (several 10^3 cp).
Figure 1 shows schematically the shape of the pressure curve and the view of the porous medium (PM) assumed to be placed in the vicinity of the well.

Core experiments

Porous media - Two porous media (outcrop from Fontainebleau - FS) are used in this work : a long one (LPM) for the main experiments and a short one for a preliminary nucleation study. They are cylindical in shape with a diameter of 4 cm and lengths of 9.6 cm (SPM) and 60 cm (LPM). Their characteristics are : oil permeability, k_o = 339 md and porosity, ϕ = 0.116. The pore volumes are 14 and 87 cm^3, respectively. These samples are resin coated, placed between two heads and connected in the set-up.

Fluids - The fluid used is a methane-dodecane mixture. The correlation between pressure and quantity of dissolved gas is measured in the laboratory. A volume Vo of dodecane is first saturated, in a recombination equipment, with methane at the absolute saturation pressure, P_{sa} = 5.06 bar. The pressure is then decreased step by step to given values of P_o. The volume of the evolved gas V_g is measured in a graduated separator and the relative volume V_R is calculated by the expression : $V_R = (V_o + V_g)/ V_o$.

Experimental device - The equipment is shown schematically in Figure 2. The porous medium is placed between several cells :

• two cells at the upstream end :

- one containing gas-free dodecane used for the saturation of the porous medium,
- the second one containing the saturated dodecane.

• the outlet of the porous medium is connected through a long thin tube to a vessel placed on an electronic balance for the monitoring of the oil produced. The vessel is finally connected to a separator in which the produced gas is collected. Two pressure taps are used for pressure drop monitoring between the inlet and the outlet face of the sample.

Procedure - The experiments are performed following two procedures :

• static experiments : the supersaturation, P_s, corresponding to a place in the vicinity of the well, is established by decreasing instantaneously the outlet pressure, down to the wanted value. The inlet valved is closed. Oil is produced as soon as bubbles are created in the porous medium. From time to time, oil equilibrated at the injection pressure, is injected during a short time lapse, (5 minutes), through the porous medium with a given pressure gradient, allowing the measurement of the oil relative permeability ;

• dynamic experiments : the reservoir conditions (Figure 1), supersaturation, P_S, mean pressure, P and pressure gradient P_{lab} are applied instantaneously by applying given inlet (mixture cell) and outlet (separator) pressures. Both valves are open and the gas-oil mixture is allowed to flow. After the time necessary to reach, by nucleation, an important gas saturation in the porous medium, the pressure gradient is increased, by increasing the inlet pressure and/or decreasing the outlet pressure. This new value is kept constant several hours

during which the produced volume of oil and gas is measured together with the saturation profile using a CT-Scanner.
The porous medium is washed with a solvent, dried and vacuum-saturated at the end of each experiment.

Micromodels
A micromodel is prepared by etching a 2-D square network pattern of pores on a glass plate, which is subsequently fused to another glass plate to create a 2-D pore network. The experimental set-up is roughly the same as the one used for the natural sandstone experiments (Figure 2). Two different saturation processes are used : one under vacuum according to [9] and the other by injection of various volumes of gas-free liquid in the micromodel initially saturated with the gas of the solution, as found in some papers [8].

EXPERIMENTAL RESULTS

Micromodels
The aim of the experiments performed in the micromodel was :
• to determine at what conditions heterogeneous nucleation takes place during a depletion process ; to show that preexistent bubbles can be easily eliminated by a careful vacuum-saturation and do not have to be accounted for as the major source of bubble creation, as it is sometimes found in the literature [8];
• to verify the heterogeneous nucleation law, allowing to use the concept of nucleation rate in a natural sandstone.
The number (Figure 3) and radius of the bubbles are measured vs time. An example is given in Figure 4a for an experiment performed with a supersaturation of 0.18 bar. It can be seen that each bubble (number 1 to 11) is formed and continues to grow at different time intervals. The extrapolated radius value for $r_b = 0$ gives the birth time of each bubble. This phenemenon is quite different from that observed in the case of experiments performed with the other saturation process (Figure 4b for various supersaturations) in which bubbles seem to be born and grow simultaneously. Moreover, the phenomenon seems to be a function of the volume of degased liquid injected for the primary saturation : 100 or 1000 PV.
The first result verifies the heterogeneous nucleation behavior and allows us to deduce the nucleation rate J from the number of bubbles formed in a unit volume, during a unit time, which is given by the slope of the linear part of each curve in Figure 3 showing the total number of bubbles created vs time.

Natural porous media
During the first stage of the experiments, oil is produced alone and the produced volume corresponds to the quantity of gas created inside the sample. After a given time lapse, gas is produced together with oil. The log-log plot of Sg vs time shows a linear part followed by a curve, due to the two-phase production when gas is also produced, reaching generally a plateau roughly proportional to the quantity of dissolved gas inside the oil. Results are given by Figure 5 for SPM.

The oil relative permeabilities (Figure 7) found for the static experiments are functions of the supersaturation; they are lower for low supersaturation than for higher ones. The contrary is observed for experiments conducted under dynamic reservoir conditions (n° 5 to 8 - Table 1) which lay roughly along a unique curve. An applied pressure gradient higher than the one corresponding to the reservoir conditions leads to the mobilization of at least a part of the gas phase.
When reservoir conditions are used, the saturation profiles (Figure 9 and 10) are generally homogeneous and can be related with the gas relative permeability. They are sometimes heterogeneous when an important pressure gradient is applied leading to the mobilization of a part of the bubbles in place. In this case, the calculation of the relative permeabilities is not done.

INTERPRETATION

Nucleation

Micromodels - It is well-known [10,11], in conditions of constant supersaturation or low pressure decline rate, that the radius of a growing bubble can be expressed by :

$$r_b = \left[2D(V_R - 1)(t - \tau_n)\right]^{\frac{1}{2}} \qquad (1)$$

using Fick's diffusion law.
This correlation is applied to the results found during the depletions performed in micromodels, knowing the diffusion coefficient, D ($3x10^{-5}$ cm^2s^{-1}), the relative volume V_R and the birth time τ_n of each bubble. Figure 4a shows that the results of this calculation agree well with the experimental results.

Natural porous media - For many bubbles, if nucleation is assumed to be a continuous phenomenon, it is possible to calculate the number and radius of bubbles born during the elapse time dt . The integration up to a given time t gives [10]:

$$S_g = \frac{8}{15}\phi\pi J \frac{V_o}{V_p}\left[2D(V_R - 1)\right]^{\frac{3}{2}}(t - \tau_1)^{\frac{5}{2}} \qquad (2)$$

The log-log plot of Sg vs time shows a linear part with a slope 5/2 verifying this calculation.
This equation is compared with experimental values of gas saturation vs time for various supersaturations (Figure 5), in an area where t is high enough to give τ values which are negligible. The value of the nucleation rate, J, is deduced, knowing the other parameters such as the relative volum V_R and the diffusion coefficient D. The value of J for each experiment (SPM and LPM) are shown vs supersaturation in Figure 6, together with results found in the literature ([10], with the same porous medium : FS and [12] with a limestone). It can be seen that :

- the nucleation rate for LPM is lower than the one found for SPM;
- both are lower than the values found previously for the same kind of porous medium (FS).

This shows that the nucleation rate is a characteristic of a given porous medium and depends on the nature of the rock cementation and roughness found on or between the grains. The usual exponential nucleation law can be applied but with parameters lower than in the case of homogeneous nucleation [13]. It is deduced that the characterization of a wellbore needs the measurement of the nucleation rate on several cores coming from the reservoir with the actual values of supersaturation. It is likely that the flow of viscous oil, even in a sand, leads

to supersaturation values in the range of 20 bar, and then to nucleation rates of some order of magnitude higher than the ones found here.

Relative permeabilities

The results found concerning relative permeabilities vs gas saturation show different behavior depending on the flow conditions i.e. with or without oil injection. The nature of the bubble population is also a parameter to be considered.

Description of the bubble population - At first, the bubble population under ***static conditions*** is described. The values of the nucleation rate, J, and of the corresponding birthtime of the first bubble τ_1 (given by 1 bubble = J V_o τ_1) allow us to describe the whole bubble population during the first stage of the depletion. As seen earlier, this period of time corresponds to the linear part of the Sg/time curves in a log-log plot. A computation already applied in a general depletion case [10] is used, but with a supersaturation remaining constant during an experiment .

• the calculation is performed in a step-by-step fashion, taking into account the total duration of the computing time, depending on the experiment duration : 400 to 10^5 s.

• during each step, nucleation of new bubbles and growth by diffusion of already created ones occur simultaneously;

• at the end of each step, the number and radius of each bubble family are calculated. The volume and the saturation of gas are then evaluated.

This computation is applied with the hypothesis that the actual supersaturation remains constant during the period of time corresponding to the nucleation. This is true as long as the

quantity of created free-gas is not too high and the quantity of oil contained in the porous medium is not too far from their initial values, so that V_o and V_R of equation (2) remain roughly constant.

Figure 8 shows values of the biggest and the smallest bubble radii vs time for each supersaturation applied in the various static experiments. It is also verified that the higher the supersaturation, the higher the number of bubbles created, but for a given gas saturation, with smaller radii as seen on Table 1 for dynamic experiments.

In our case, the shape of the gas clusters which are relatively small is assumed to be roughly spherical, contrary to the shape of very large ones (up to 10 cm) obtained in a limestone. In this last case, the radius of a bubble has to be replaced by the length, along flow direction, of the cluster measured by specific experiments[10].

The effect of the reservoir conditions on the bubble population is now considered in terms of the ***pressure gradient*** P_{inj} applied in connection with the one found at a given place in the reservoir at a distance R from the well. On the other hand, a simple calculation based on the comparison of the viscous and the capillary forces [10,16] allows us to find out the minimum pressure gradient, P_{mob} able to mobilize a bubble of given radius. These pressure gradient values are shown in Table 1.

The comparison of these pressure gradients and the CT-Scanner saturation profiles measured during the various experiments leads to deduce that (Figure 9 and 10) :

• there is a good agreement between the calculated and experimentally observed values of P_{mob}. Many examples can be given, showing that the calculated value of P_{mob} based on the bubble radius represents really the ability for the bubbles to be mobilized, and that an applied presure gradient lower than this value let the bubbles stranded (Figure 9 - bottom) whereas a pressure gradient just higher is able to mobilize the bubble population (Figure 9 - top) ;
• during the static experiments, the volume of oil injected is too small to have an important displacement of the gas phase. Then the relative permeabilities measured correspond to the flow of oil in presence of the calculated bubble population : large bubbles in the case of low supersaturation, small ones if the supersaturation is high enough. The effect of bubble radius is shown for example in the case when a high value of P_{inj}, 4.06 bar, cannot mobilize an important part of the gas in place (Figure 10 - bottom);
• for reservoir conditions, no change in the saturation profile shape was observed. The pressure gradient applied, far lower than the mobilization pressure gradient (Table 1), is likely able to sweep only the gas saturation peaks. The largest gas clusters are mobilized and divided into daughter-bubbles [scission probability like in the case of oil blobs : 17,18] which remain stranded. The bubble population is then homogeneous, similar to the population obtained with a high supersaturation (4.06 bar), leading to the same correlation k_{ro} / S_g ;
• for conditions of higher pressure gradient than actually applied in the reservoir the whole population may be mobilized. This can be the behavior observed in our reservoir if the production rate is increased.

CONCLUSION

The results of this work lead to a procedure for estimating the relative permeabilities necessary to optimize the oil production of a given well, the pressure of which is lower than the saturation pressure of the oil.
• At first, the conditions prevailing in the wellbore region are determined in terms of distance from the well in connection with the actual well productivity. Depending on the productivity characteristics (flowrate and oil viscosity), it is shown that supersaturation may reach several bar and it can be assumed that the flow of viscous oil leads to higher supersaturations ;
• The derived experimental conditions are applied to experiments performed within actual rock-fluid system and constant supersaturation values ;
• The experiments concerned with nucleation phenomena and injection performance show that :

- the nucleation rate is a parameter sensitive to the rock-fluid system. Therefore, nucleation tests on several cores coming from the wellbore are mandatory. At the end of the nucleation period with a constant supersaturation, the gas clusters invading the porous medium may have a large radius distribution lying between some millimeters and some centimeters ;
- the oil relative permeability is not a function of the gas saturation alone, but also of the nature of the bubble population, which plays an important role ;

This is explained by the effect of the pressure gradient applied which can either make the bubble radius distribution uniform but immobile or sweep the whole bubble population.

The above observations lead to the understanding of the low oil productivity when the pressure in the vicinity of the well has fallen below the saturation pressure, and thus may be used to optimize the production.

NOMENCLATURE

D	molecular diffusion coefficient, cm^2s^{-1}
J	nucleation rate, bubble $cm^{-3}s^{-1}$
k	permeability, 1 darcy = 10^{-8} cm^2
k_{ro}	oil relative permeability
N_b	number of created bubbles
PM	porous medium
P_o	oil pressure
P_s	absolute pressure, bar
PV	pore volume, cm^3
r_b	bubble radius, cm
S_{gc}	critical gas saturation
V_g	gas volume, cm^3
V_o	oil volume, cm^3
V_R	relative volume = (Vo+Vg)/Vo
P_{inj} or P_{lab}	pressure drop applied on the porous medium, bar
P_{mob}	pressure drop able to mobilize a given bubble size, bar
P_S	supersaturation pressure, bar
ϕ	porosity
$\tau_1..\tau_n$	birth time of the first ....the n^{th} bubble, s

REFERENCES

1. Maini, B.B.: "Is it Futile to Measure Relative Permeability for Heavy Oil Reservoir?" paper 95-97 presented at the 46th Annual Technical Meeting of the Petroleum Society of CIM, Banff, AB, (1995).
2. Stewart, C.R., Hunt Jr, E.B., Schneider, F.N., Geffen, T.M. and Berry Jr. V.J.: "The role of bubble formation in oil recovery by solution gas drives in limestones" *Petr. Trans. AIME* (1954) vol. 201.
3. Kortekaas, T.F.M. and van Poelgeest, F.:"Liberation of Solution Gas During Pressure Depletion of Virgin Watered-Out Oil Reservoirs" SPERE (1991) 329-35.
4. Firoozabadi, A., Ottensen, B. and Mikkelson, M.: "Measurements of supersaturation and critical gas saturation". *Paper SPE RE* 19694 (1992) p. 337-344.
5. Kamath, J. and Boyer, R.E.: "Critical gas saturation and supersaturation il low permeability rocks". SPE n° 26663, *68th Annual Technical Conference and Exhibition*, Houston (1993).
6. Moulu, J.C. and Longeron, D.: "Solution gas-drive : Experiments and simulation". Paper presented at the *Fifth Europ. Symp. on improved oil recovery*. Budapest (1989).
7. Sheng, J. J. " Foamy Oil Flow in Porous Media" Ph. D. dissertation, U. of Alberta (1997).
8. El Yousfi.A, Zarcone.C, Bories.S and Lenormand.R : "Physical mechanisms for bubble growth during solution gas drive", Paper SPE 38921 presented at the 1997 SPE An Tech Conf and Exh held in San Antonio, TX, October 5-8, 1997.
9. Betata, S. A.:" Les écoulements polyphasiques aux abords des puits dans les gisements d'hydrocarbures" Ph D, U. of Paris VI (1997).
10. Moulu, J.C.: "Solution gas-drive : Experiments and simulation" *Journal of Petr. Sci. Eng* (1989), 2, page 379-386, Feb. 1989.
11. Hong, J. and Woo, H.S.: "Application of the fractional derivates method to bubble growth/dissolution processes with or without first-order chemical reaction", *AIChE journal* (1985) Vol. 31 N° 10.
12. Wieland, D.R and Kennedy, H.T : "Measurements of bubble frequency in cores" *Petr. Trans. AIME* (1957) vol. 210.
13. Blander, M. and Katz, J.L.: "Bubble nucleation in liquids". *AIChE Journal* (1975) vol. 21, N° 5.
14. Yortsos, Y.C. and Parlar, M.: "Phase change in binary systems in porous media" Paper SPE 19697 presented at the 64th An Tech Conf and Exh held in San Antonio, TX, Oct. 8-11, 1989.
15. Du, C. and Yortsos, Y.C.: " A Numerical Study of the Critical Gas Saturation in a Porous Medium" (1997) Submitted to Transport in Porous Media.

16. Madaoui, K.: "Condition de mobilité de la phase gazeuse lors de la décompression d'un mélange d'hydrocarbures en milieu poreux". Ph D, U. of Toulouse 1975.
17. Payatakes, A.C. and Dias, M.M.:" Immiscible Microdisplacement and Ganglion Dynamics in Porous Media" Rev. in Chem. Eng., 2, 85 (1984).
18. Moulu, J.C.: "Behaviour of oil ganglia displaced by surfactant solution in a porous medium" *J. Physique lett.* (1985) 46.

Table 1 - Experimental and mobilization conditions during the dynamic experiments

N° Exper.	**P $_s$** (bar)	**P $_{inj.}$**(bar) experimental	N_b - **r$_b$** (cm)	**P $_{mob.}$** (bar) calculated
5	2.5	0.065 (well) up to 1.6	*50* - 0.83 0.97	2.0 1.7
6	2.5	0.065 (well) up to 2.0	*50* - 0.83 0.97	2.0 1.7
7	3	0.4 (well) up to 1.2	*200* - 0.66 0.8	2.5 2.0
8	3.4	0.85 (well) up to 2.0	*500* - 0.5 0.63	3.3 2.6

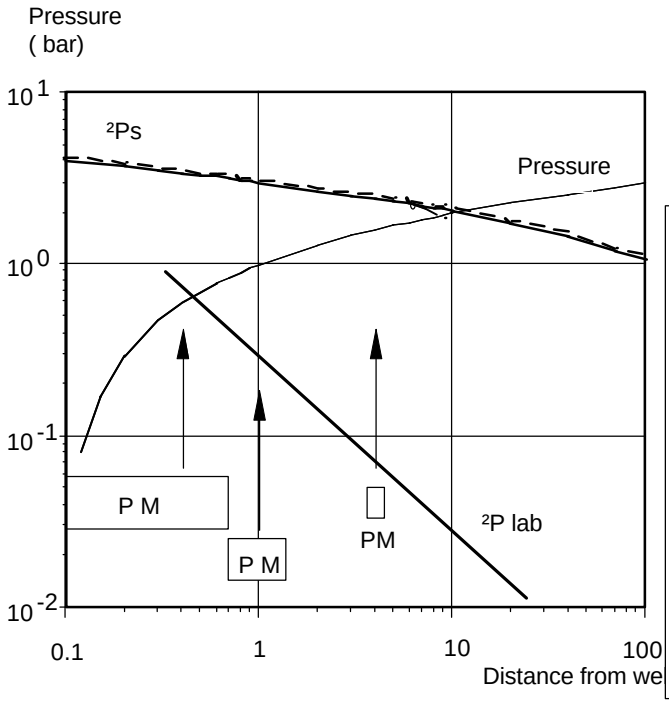

Figure 1 - Wellbore region description. Pressure and supersaturation profiles. Places where the porous medium (PM) is assumed to be during the experiments : 0.4 -1.0 and 4.0 m from the well

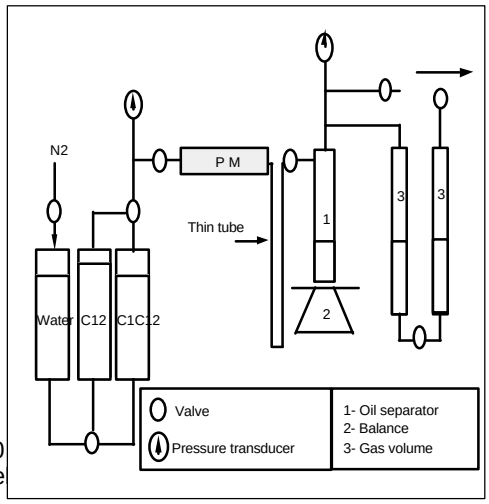

Figure 2 - Experimental set-up

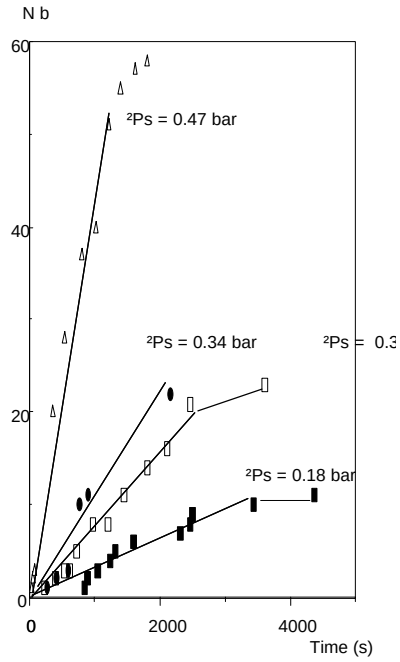

Figure 3 - Number of bubbles created vs time for various supersaturation values.

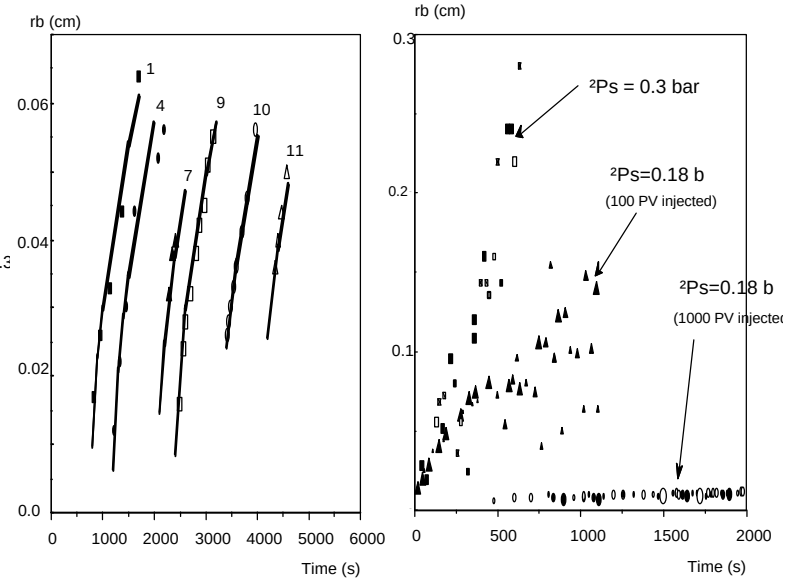

a) b)

Figure 4 - a) Radius of 11 bubbles showing a separate birth time for each one. Supersaturation = 0.18 bar (points : experiments; curve : calculation by Equ.1) - b) Radius of preexistent bubbles vs time for two supersaturation values. The effect of the volume injected during the initial saturation is also shown.

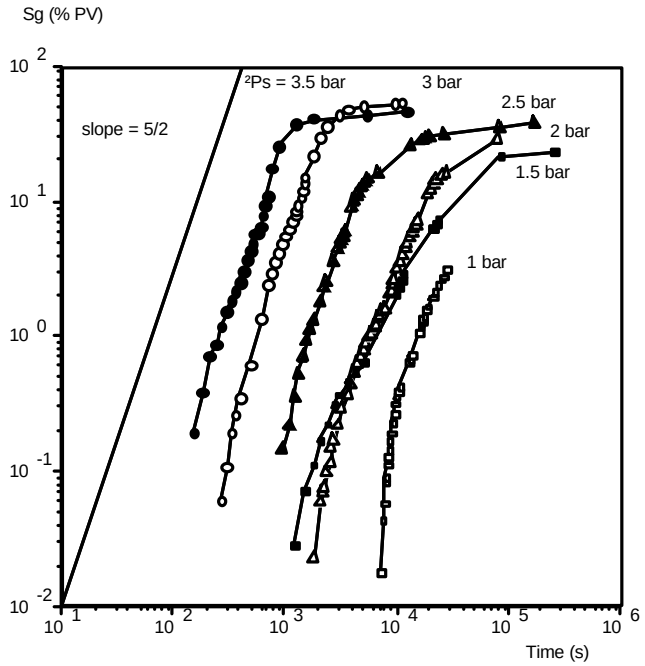

Figure 5 - Gas saturation measured vs time for various supersaturations. Points = experiments. Curves = fit of the curves with Equ.2 and by adjusting J.

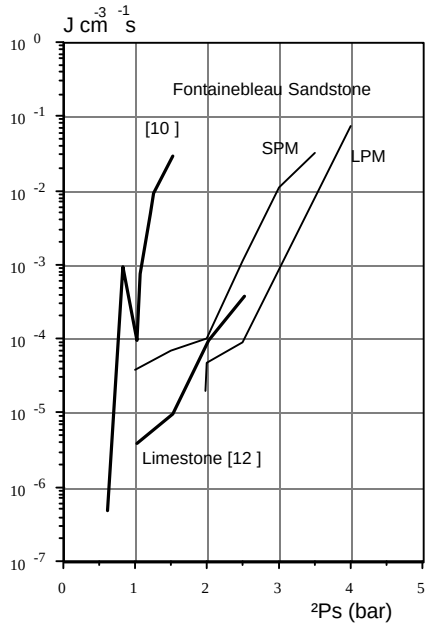

Figure 6 - Nucleation rate as a function of supersaturation for various porous media.

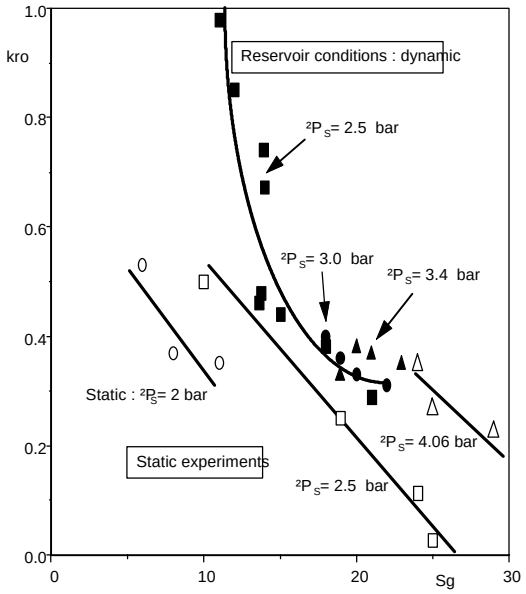

Figure 7 - Oil relative permeabilities : separate curves for static experiments and a unique curve for dynamic (reservoir) conditions.

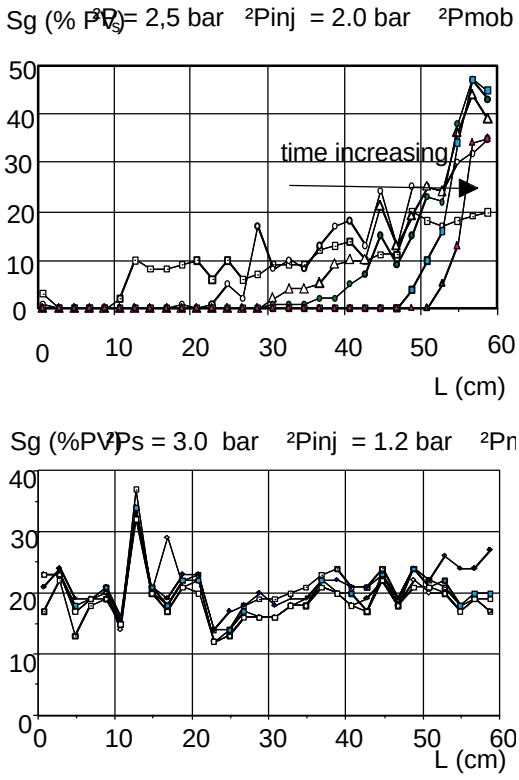

Figure 9 - Dynamic experiments - Mobilization or profile not modified depending on the pressure gradient applied. Curves for times up to 5 hours.

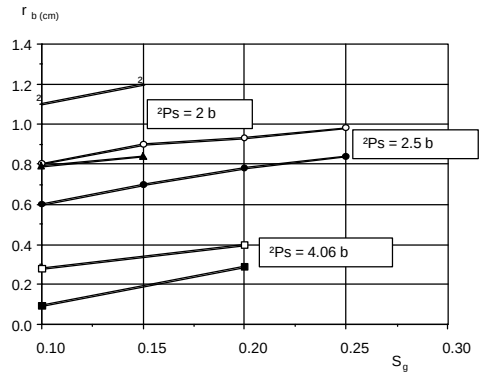

Figure 8 - Radius of the bubbles during several static experiments. For each supersaturation value, the radius of the biggest and of the smallest bubbles is given.

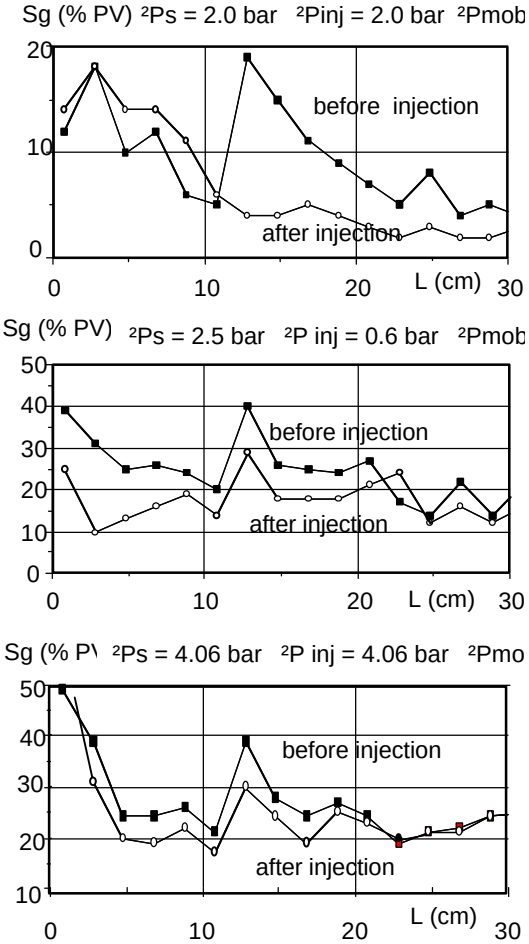

Figure 10 - Static experiments with various conditions. Effect of the bubble radius.